9-1-2011

Compact binaries in star clusters - II. Escapers and detection rates

J. M.B. Downing

M. J. Benacquista

M. Giersz

R. Spurzem

Recommended Citation

J. M.B. Downing, et. al., (2011) Compact binaries in star clusters - II. Escapers and detection rates.Monthly Notices of the Royal Astronomical Society416:1133. DOI: http://doi.org/10.1111/j.1365-2966.2011.19023.x

Monthly Notices
of the
ROYAL ASTRONOMICAL SOCIETY

Mon. Not. R. Astron. Soc. **416,** 133–147 (2011) doi:10.1111/j.1365-2966.2011.19023.x

Compact binaries in star clusters – II. Escapers and detection rates

J. M. B. Downing,[1⋆] M. J. Benacquista,[2] M. Giersz[3] and R. Spurzem[1,4,5]

[1]*Astronomisches Rechen-Institut, Zentrum für Astronomie der Universität Heidelberg, Mönchhofstraße 12-14, D-69120 Heidelberg, Germany*
[2]*Center for Gravitational Wave Astronomy, University of Texas at Brownsville, Brownsville, TX 78520, USA*
[3]*Nicolaus Copernicus Astronomical Center, Polish Academy of Sciences, ul. Bartycka 18, 00-716 Warsaw, Poland*
[4]*National Astronomical Observatories, Chinese Academy of Sciences, 20A Datun Rd., Chaoyang District, Beijing 100012, China*
[5]*Kavli Institute of Astronomy and Astrophysics, Peking University, Beijing 100871, China*

Accepted 2011 May 5. Received 2011 April 29; in original form 2010 August 30

ABSTRACT

We use a self-consistent Monte Carlo treatment of stellar dynamics to investigate black hole binaries that are dynamically ejected from globular clusters in order to determine if they will be gravitational wave sources. We find that many of the ejected binaries initially have short periods and will merge within a Hubble time due to gravitational wave radiation. Thus they are potential sources for ground-based gravitational wave detectors. We estimate the yearly detection rate for current and advanced ground-based detectors and find an enhancement over the rate predicted for binaries produced by pure stellar evolution in galactic fields. We conclude that, in agreement with previous studies, including globular cluster populations is essential for calculating the correct merger detection rates for gravitational wave detection.

Key words: gravitational waves – binaries: close – globular clusters: general – galaxies: star clusters: general.

1 INTRODUCTION

Gravitational waves, metric perturbations in space–time caused by time-varying mass–energy distributions, offer a new window on the Universe that is independent of the electromagnetic spectrum. In particular, the inspiral and merger of stellar mass compact binaries [binaries consisting of neutron stars (NSs) and/or black holes (BHs)] are predicted to be major burst sources for the high-frequency ground-based gravitational wave detectors Virgo and Laser Interferometer Gravitational Wave Observatory (LIGO). The current generation of these detectors should be able to detect such events out to the Virgo cluster (Abbott et al. 2005, 2006, 2010), while upgrades to these detectors (e.g. advanced Virgo) should lead to detections at cosmologically significant distances. At larger separations, compact binaries, including white dwarf (WD) binaries, within the Galaxy may be detected by the low-frequency space-based gravitational wave detector Laser Interferometer Space Antenna (LISA) planned for 2018–2020 (Hils, Bender & Webbink 1990; Benacquista 2001; Nelemans, Yungelson & Portegies Zwart 2001; Belczynski, Benacquista & Bulik 2010). In particular, WD–WD binaries are expected to be plentiful and will manifest as a confusion-limited noise source (Evans, Iben & Smarr 1987; Hils et al. 1990; Nelemans et al. 2001; Timpano, Rubbo & Cornish 2006; Ruiter et al. 2010).

It is possible to place some constraints on the number of NSs and NS–NS binaries using pulsar observations and gamma-ray bursts (Kalogera et al. 2004; Lorimer 2008). However, many of the sources producing gravitational waves (particularly BH–BH binaries) will not emit significant amounts of electromagnetic radiation, and it is necessary to perform population synthesis models in order to constrain event rates and produce templates for gravitational wave detectors. Significant efforts have been made to constrain the population of compact binaries in galactic fields (e.g. Portegies Zwart & Yungelson 1998; Fryer, Woosley & Hartmann 1999; Belczynski, Kalogera & Bulik 2002; Belczynski et al. 2007), and these studies predict that detection rates will be dominated by NS–NS inspirals. Although BH–BH binaries are more massive and can be detected with a higher signal-to-noise ratio at larger distances, NSs are more plentiful due to the power-law shape of the initial mass function (IMF) and the progenitors of NS–NS binaries are less likely to undergo mass transfer leading to a merger than are their BH–BH counterparts. In particular, Belczynski et al. (2007) have estimated advanced LIGO detection rates of $\sim 20\,\mathrm{yr}^{-1}$ for NS–NS binaries, $\sim 2\,\mathrm{yr}^{-1}$ for BH–BH binaries and only $\sim 1\,\mathrm{yr}^{-1}$ for NS–BH binaries. Belczynski et al. (2010) have studied the possibility that stellar mass compact binaries may be individually resolved by LISA rather than simply appearing as a noise source. They have determined that there will only be a small number of resolved stellar mass objects in the LISA band and that more than half of these will be NS–NS binaries.

Although BH–BH binaries may be rare in galactic fields, it is possible to produce such binaries through dynamical interactions in star clusters (Sigurdsson & Phinney 1993). There are two types of interaction that create BH–BH binaries. The first is few-body binary formation where a close encounter between multiple stars transfers kinetic energy to one star at the expense of the relative energy between two others. This leaves a bound pair and an escaper. The

⋆E-mail: downin@ari.uni-heidelberg.de

second is exchange where a single star interacts with a binary and is swapped with one of the original binary members. Due to equipartition of energy, both of these processes favour the escape of the lightest member of the interaction (Hills & Fullerton 1980; Heggie, Hut & McMillan 1996) and thus preferentially introduce massive objects, such as BHs, into binary systems. Another important effect is binary hardening where 'hard' binaries (binaries with a binding energy greater than the kinetic thermal energy of the cluster) can have their binding energy increased and thus their period shortened (Heggie 1975). This process reduces the separation between the binary members and can accelerate the evolution of a BH–BH binary towards the gravitational radiation-dominated regime. Interactions between binaries can result in both exchange and binary hardening for both binaries. Finally, interactions can destroy binaries if the kinetic energies of the centres of mass are high enough. All of these processes are enhanced by high stellar densities and proceed most rapidly in the very concentrated cores of star clusters. Equipartition of energy requires that the most massive objects in a star cluster sink to the centres in a process called mass segregation (Spitzer 1987). Since BHs and binaries rapidly become the most massive objects in the system, they will rapidly migrate to the centre of the cluster where interaction rates are highest. This means that BHs will tend to experience a disproportionately large number of interactions, further enhancing the effect of star cluster dynamics on the BH–BH binary population.

The effect of star cluster dynamics on BH–BH binary populations has been studied before using limited dynamical models. Gültekin, Miller & Hamilton (2004) and O'Leary et al. (2006) have investigated the BH–BH binary population in star clusters assuming the BHs form a completely mass-segregated subsystem that interacts only with itself. They find that the BHs interact strongly with each other leading to both the formation and destruction of BH–BH binaries. Depending on the initial conditions assumed for their clusters, O'Leary et al. (2006) find ∼1–10 BH–BH merger detections per year using the parameters for advanced LIGO. Up to 70 per cent of these mergers occur in BH–BH binaries that have been dynamically ejected from the clusters. These simulations contained no treatment of stellar evolution. By contrast, Sadowski et al. (2008) have performed cluster simulations with stellar evolution but assuming that the BHs and BH–BH binaries always remain in dynamical equilibrium with the rest of the cluster. This is in some sense the opposite dynamical assumption made in O'Leary et al. (2006) and leads to a much higher merger rate of ∼25–3000 detections per year, depending again on the initial conditions. This is because although there are fewer interactions that form BH–BH binaries, once formed such a binary is unlikely to interact with another BH and be disrupted. They claim only ∼10 per cent of mergers occur outside their clusters. Finally, both Portegies Zwart & McMillan (2000) and Banerjee, Baumgardt & Kroupa (2010) have performed direct *N*-body simulations of star clusters focusing on BHs and the BH–BH binary population. These simulations include full cluster dynamics but contain fewer stars than a real globular cluster. Portegies Zwart & McMillan (2000) find a detection rate of a few detections per year to almost one a day depending on the assumed globular cluster formation history and the composition of the globular cluster population. They also find that the vast majority of the BH–BH binaries are ejected from the cluster and thus most mergers occur in the field. Their detection rates are between those of Sadowski et al. (2008) and O'Leary et al. (2006), but the small number of mergers in the cluster are more consistent with the O'Leary et al. (2006) result. The somewhat large simulations of Banerjee et al. (2010) confirm this picture although they do not include stellar evolution and use a rather simplified stellar mass function. They find a detection rate about an order of magnitude lower than Portegies Zwart & McMillan (2000), but an order of magnitude higher than O'Leary et al. (2006). They attribute this to differences in the type of clusters being simulated rather than to the fundamental differences of methodology.

In (Downing et al. 2010, hereafter Paper I), we revisited this problem using a Monte Carlo star cluster simulation code that includes stellar evolution, a fully self-consistent treatment of the global cluster dynamics, and is capable of simulating a number of particles comparable to real globular clusters. We demonstrated that the BHs strongly mass segregate and thus confirm that the approximation made in O'Leary et al. (2006) is favoured over that of Sadowski et al. (2008). We found several potential LISA sources in our simulations, some of which would be detectable in nearby globular clusters. Our results differ from O'Leary et al. (2006), in that we find no BH–BH mergers within our clusters, possibly due to our more approximate treatment of few-body interactions. This result is, however, consistent with the direct *N*-body results of Portegies Zwart & McMillan (2000) and Banerjee et al. (2010). In Paper I we found that many BH–BH binaries were ejected from the cores of our clusters with very high binding energies, consistent with the results of both Portegies Zwart & McMillan (2000) and O'Leary et al. (2006). These binaries are massive enough and have short enough periods that they should merge in a galactic field within a Hubble time ($T_{\rm H}$). Investigating these escaping binaries is the subject of this paper. In Section 2 we briefly describe our Monte Carlo code and initial conditions. In Section 3 we describe the properties of the escaping binaries. In Section 4 we consider the merger rate of escaping binaries, and we translate this into a detection rate for ground-based gravitational wave detectors in Section 5. We discuss our results in Section 6 and conclude in Section 7.

2 METHODS AND SIMULATIONS

Here we briefly outline our numerical methods and initial conditions. We base our results on the simulations described in Paper I, and the interested reader is referred there for further details.

2.1 The Monte Carlo code

We simulate star clusters using a Hénon-type Monte Carlo code (Hénon 1971) with improvements for both global and binary dynamics developed by Stodółkiewicz (1982) and Stodółkiewicz (1986) as incorporated by Giersz (1998). In this code, star clusters are assumed to be spherically symmetrical with their global dynamical evolution governed by two-body relaxation. Using this approximation, the orbits of individual stars can be described as plane rosettes defined by their energy, E, and angular momentum vector, $\boldsymbol{J}$. The dynamical evolution of the cluster over a time Δt can then be calculated using an appropriate scattering angle chosen by Monte Carlo sampling from the theory of two-body relaxation. This method has the advantage of requiring only a fixed number of operations per particle and thus scaling as $\mathcal{O}(N^{1-2})$, where N is the number of particles in the simulation, as opposed to the $\mathcal{O}(N^{3-4})$ of direct *N*-body simulations. This allows us to run simulations with 10^5–10^6 particles, similar to the number of stars in real globular clusters, while still being able to perform large parameter space studies.

Strong few-body interactions are not part of the Monte Carlo approximation and are modelled separately by incorporating cross-sections for such events to occur and prescriptions to determine their

outcomes. The probability of three-body binary formation is calculated according to the prescription found in Giersz (2001), which is in turn based on the work of Heggie (1975) and Stodółkiewicz (1986). The cross-sections for binary–single and binary–binary interactions are calculated following the method of Giersz & Spurzem (2003). The outcome of binary–single interactions are determined by the formulae given in Giersz (1998). The outcomes of binary–binary interactions are based on the numerical few-body scattering experiments of Mikkola (1983a,b, 1984a,b) as implemented by Stodółkiewicz (1986). The probabilities for exchanges during binary–single and binary–binary interactions are taken from Heggie et al. (1996). In 12 per cent of cases a binary–binary interaction results in two binaries on a hyperbolic orbits, while the remaining 88 per cent of cases result in one binary and two escapers. Triple formation is not an outcome allowed by any of our prescriptions since there exists no analytical formalism to describe the long-term evolution of triple systems.

The code includes treatments for single and binary stellar evolution using the Single Stellar Evolution (SSE) (Hurley, Pols & Tout 2000) and Binary Stellar Evolution (BSE) (Hurley, Tout & Pols 2002) packages (Giersz, Heggie & Hurley 2008). These packages include prescriptions for stellar and binary evolution from the zero-age main sequence to the stellar remnant at a variety of metallicities and include analytic treatments of mass transfer and perturbed evolution in binary systems. For our purposes, the primary effect of metallicity is higher mass BHs at low metallicity due to less efficient line driving of stellar winds on the giant and asymptotic giant branch (Belczynski et al. 2002). A study of the resulting BH mass distributions is given in Belcyznski et al. (2006). Prescriptions for natal kicks in supernovae remnants (Lyne & Lorimer 1994) are also included. They are drawn from a Maxwellian distribution with a peak centred at $190\,\mathrm{km\,s^{-1}}$ based on the proper motion studies of Hansen & Phinney (1997). For the BHs, these kicks are then reduced in proportion to the mass of material accreted during fallback as calculated in Belczynski et al. (2002). The Hansen & Phinney (1997) kick distribution is rather old, and more recent works favour a Maxwellian with a peak at $\sim 265\,\mathrm{km\,s^{-1}}$ (Hobbs et al. 2005). We note that both of these distributions have peaks well above the escape velocity of any of our simulations ($<50\,\mathrm{km\,s^{-1}}$ at the half-mass radius). Thus the only thing keeping a substantial number of BHs in our clusters is the Belczynski et al. (2002) fallback reduction. The fallback reduction is kick-independent and, for the most massive BH progenitors, can reduce the kicks to zero. We do not expect that choosing one or other of the realistic kick distributions will strongly affect our results. An estimate for the gravitational wave inspiral time-scale based on the quadrupole approximation (Peters 1964) is included for compact binaries. Tidal truncation of the cluster is treated using the prescriptions of Baumgardt (2001) (Giersz 2001; Giersz et al. 2008).

The code agrees well with direct N-body simulations in the case of equal masses (Giersz 1998), a mass function (Giersz 2001, 2006) and when stellar evolution has been included (Giersz et al. 2008). Simulations using this code have also been shown to reproduce the physical parameters of the observed star clusters M67 (Giersz et al. 2008), M4 (Giersz & Heggie 2008) and NGC 6397 (Giersz & Heggie 2009). Despite these successes the code has some limitations. Of particular interest for our study is the Spitzer instability (Spitzer 1987) where massive objects, such as BHs, can fall out of energy equipartition and form a strongly interacting subsystem in the cluster core. In such a situation, the assumption of weak scattering may no longer hold and the Monte Carlo approximation can break down. Heggie & Giersz (2009) have compared the behaviour of the core region of Monte Carlo and direct N-body simulations of NGC 6397 and have found good agreement between both sets of simulations in the binary binding energies and escape rates. This indicates that core dynamics are being reproduced properly. Artificially small bound subsystems can also be detected by sudden drops in the central potential of the cluster. None of our simulations demonstrates such an effect, indicating that there is no major unphysical behaviour in the cluster cores. Finally we showed that the binding energy of the escapers was in good agreement with that found in O'Leary et al. (2006) and Portegies Zwart & McMillan (2000), indicating that the energetics of binaries in the core are being treated accurately.

A more serious concern is the lack of direct few-body integration in our binary–single and binary–binary interactions. This reduces the number of possible outcomes for these interactions and eliminates the possibility of mergers during the interaction. Another problem is that there is no analytic formula that can be easily used to calculate eccentricities at the end of few-body interactions, and for this reason the few-body prescriptions do not update eccentricities in any interactions other than three-body binary formation (where eccentricity is chosen randomly) or sometimes in exchanges (where it is set to zero). Since most interactions tend to induce eccentricity in binaries, the eccentricities produced by the code will be systematically underestimated. If, for example, a binary were circularized by stellar evolutionary effects and then had BHs exchanged into it, the result would be a circular rather than eccentric. To control for this, we repeat the analysis for all our BH–BH binary escapers while replacing the eccentricity at ejection given by the code with an eccentricity drawn from a thermal distribution [$f(e) = 2e$]. The thermal distribution favours higher eccentricities, so by comparing the results produced by these two distributions we should be able to constrain the error made by the Monte Carlo code. In particular, since gravitational wave radiation can be strongly enhanced at high eccentricities, we expect the thermal distribution to produce faster inspirals and hence a larger merger rate.

2.2 Initial conditions

The initial conditions for our simulations were described in Paper I and we merely summarize them here. Our results are based on a set of 160 simulations, each with $N = 5 \times 10^5$ particles, a Kroupa power-law IMF (Kroupa, Tout & Gilmore 1993) with a lower slope of $\alpha_l = 1.3$, an upper slope of $\alpha_l = 2.3$, a break mass of 0.5 $\mathrm{M}_\odot$ and masses between 0.1 and 150 $\mathrm{M}_\odot$. The models are initialized with Plummer profiles with a tidal radius of $r_\mathrm{t} = 150\,\mathrm{pc}$. We have used two initial binary fractions (f_b), 10 and 50 per cent, with initial binary parameters taken from Kroupa (1995). We use two metallicities, $Z = 0.02$ (solar) and $Z = 0.001$ (low). Finally, we use four different initial concentrations defined by the ratio of the tidal radius to the initial half-mass radius (r_h), $r_\mathrm{t}/r_\mathrm{h} \in 21, 37, 75, 180$, corresponding roughly to initial number densities within the half-mass radius of 10^2, 10^3, 10^4, $10^5\,\mathrm{pc}^{-3}$. Smaller half-mass radii reduce the half-mass relaxation time, given by Spitzer (1987), as

$$t_\mathrm{rh} = 0.138 \frac{N^{1/2} r_\mathrm{h}^{3/2}}{\langle m \rangle^{1/2} G^{1/2} \ln \gamma N}, \quad (1)$$

where $\langle m \rangle$ is the average mass in the system, G is Newton's gravitational constant and $\gamma = 0.02$ is an empirically determined constant, in the highest concentration clusters and thus leads to faster dynamical evolution. Taken together, these yield 16 possible combinations of initial conditions. We have performed 10 independent realization of each set of initial conditions in order to constrain statistical

Table 1. The number of BH–BH binaries that escape from the cluster and the number of BH–BH mergers. The first column identifies the initial conditions. The second column gives the total number of BH–BH binary escapers summed over all 10 independent realizations of each simulation. The third column gives the number of BH–BH escapers averaged over all 10 independent realizations. The fourth column gives the number of BH–BH escapers that merge within a Hubble time summed over all 10 independent realizations. The fifth column gives the number of BH–BH escapers that merge, averaged over all 10 independent realizations. The sixth and seventh column are the same as the fourth and fifth except that the eccentricity on ejection given by the Monte Carlo code has been replaced by one drawn from a thermal distribution. The uncertainty in columns three, five and seven is the rms scatter across the 10 independent realizations.

	BH–BH escapers					
Simulation	N_E	$\langle N_E \rangle$	N_M	$\langle N_M \rangle$	$N_{M,\mathrm{eth}}$	$\langle N_{M,\mathrm{eth}} \rangle$
10sol21	242	25 ± 3	2	1 ± 1	6	1 ± 1
10sol37	436	44 ± 2	6	1 ± 1	16	2 ± 2
10sol75	518	52 ± 3	26	3 ± 2	63	7 ± 4
10sol180	646	65 ± 5	119	12 ± 2	264	27 ± 3
50sol21	54	6 ± 2	1	1 ± 1	1	1 ± 1
50sol37	193	20 ± 5	2	1 ± 1	9	1 ± 1
50sol75	408	41 ± 4	21	3 ± 2	50	5 ± 2
50sol180	672	60 ± 7	115	12 ± 2	246	25 ± 5
10low21	707	71 ± 5	5	1 ± 1	18	2 ± 2
10low37	958	96 ± 5	19	2 ± 2	48	5 ± 2
10low75	1185	119 ± 6	60	6 ± 3	141	15 ± 3
10low180	1315	132 ± 6	251	26 ± 6	476	48 ± 4
50low21	283	29 ± 6	7	1 ± 1	8	1 ± 1
50low37	522	53 ± 5	21	3 ± 2	31	4 ± 2
50low75	888	89 ± 6	68	7 ± 3	115	12 ± 3
50low180	1225	123 ± 2	245	25 ± 5	415	42 ± 5

fluctuations for a total of 160 individual simulations. We confirmed that 10 simulations are sufficient for accurate statistics. The initial conditions are summarized in table 1 of Paper I. For the simulation IDs in the first column, the first number gives the binary fraction, the three letter code designates solar (sol) or low (low) metallicity and the last number gives the initial concentration. The simulations have been performed on the Höchst Leistungs Rechenzentrum Stuttgart (HLRS) supercomputer in Stuttgart. Each is run on a single processor and it takes between 4 and 24 h to simulate a cluster for $1\,T_{\mathrm{H}}$.

3 PROPERTIES OF ESCAPING BINARIES

In Paper I we discovered no BH–BH mergers within our clusters although we found a few potential LISA sources. We found, however, that many of our clusters ejected hard BH–BH binaries with binding energies $>1000\,k_{\mathrm{B}}T$, where $k_{\mathrm{B}}T = M_{\mathrm{core}}\sigma^2_{\mathrm{core}}/2N_{\mathrm{core}}$ is the thermal energy in the core of the cluster, M_{core} is the total mass of the core, N_{core} is the number of stars in the core and σ_{core} is the velocity dispersion in the core. This result is consistent with the binding energy distribution found by both Portegies Zwart & McMillan (2000) and O'Leary et al. (2006). We speculated that these hard binaries may merge within a Hubble time and be sources of gravitational waves for both ground- and space-based detectors.

In Table 1 we present the number of escapers from each of our simulation both summed and averaged over all 10 independent realizations. The trends in Table 1 follow similar trends to those found for the formation of BH–BH binaries in table 3 of Paper I, namely more BH–BH escapers at higher initial concentration and at low metallicity. The trend with initial concentration is clear; at higher density there are more interactions per unit time and hence more dynamical BH–BH binary formation and ejection over $1\,T_{\mathrm{H}}$. The trend with metallicity is due both to the larger number of BHs and their greater mass at low-Z. The mass-segregation time-scale governing how quickly massive objects sink to the cluster centre is given by

$$t_{ms} \propto t_{\mathrm{rh}} \frac{m_2}{m_1}, \tag{2}$$

where $m_1 > m_2$ (Watters, Joshi & Rasio 2000; Khalisi, Amaro-Seoane & Spurzem 2007). Thus the more massive BHs and BH–BH binaries in low-metallicity clusters mass segregate faster, and dynamical evolution is accelerated. Strangely, there seem to be fewer BH–BH escapers at higher f_{b} even though there are more BHs and more binaries for them to be exchanged into. This seemingly paradoxical behaviour is due to the fact that the Kroupa (1995) binary prescriptions create many soft binaries that are quickly disrupted and initially increase the number of centres of mass in the system. This in turn increases the relaxation time in physical units (see equation 1) which leads to slower dynamical evolution and hence fewer dynamically formed binaries. This effect is discussed further in an erratum to Paper I. Column 2 of Table 1 shows that that there is very little simulation-to-simulation scatter in the number of BH–BH binaries ejected.

Fig. 1, which gives the number of BH–BH escapers per Gyr relative to the start of the simulation from which they escaped, confirms this picture. There are more BH–BH escapers at high initial concentration, lower metallicity and lower f_{b}. Fig. 1 also demonstrates the effect the initial conditions have on the time and rate at which BH–BH binaries escape from the simulations. For low initial concentrations the escape of BH–BH binaries does not commences immediately and, when it does, it proceeds at a slow, fairly constant rate. By contrast, at high initial concentrations there is a large burst of escapers very early but the escape rate drops off later in the life of the cluster. This is due to the shorter relaxation time at higher concentrations. The trend is enhanced at lower metallicity, due to the shorter mass-segregation time-scales in these clusters. Therefore low-concentration, high-metallicity clusters produce fewer ejections within a Hubble time than do high-concentration, low-metallicity clusters. The clusters with a higher initial binary fraction produce a peak that is lower, later and more extended than those with a lower initial binary fraction. This again reflects the slower relaxation in these clusters. In Fig. 2 we present the total number of escapers summed over all 160 simulations and binned per Gyr assuming all clusters form at the same time. It is apparent that the escape rate will be highest early in the life of the cluster population where it is dominated by low-metallicity, high-density clusters, but that there will be an appreciable number of escapers at late times as well.

In Fig. 3 we present the eccentricity distribution of BH–BH binaries at the moment of escape. In Section 2.1 we described how eccentricities may be underestimated and how we control for this by repeating the analysis with eccentricities drawn from a thermal distribution. Fig. 3 shows how these distributions differ and in particular that the Monte Carlo eccentricities show a large peak at $e = 0$. As described in Section 2.1, this peak is primarily the result of binaries circularized during stellar evolution not having the eccentricities updated during interactions. By comparing the results given by these two distributions we should be able to constrain the effect of eccentricity on our predicted detection rates.

Fig. 4 gives the period distribution of all escaping binaries. All periods are short with few more than a year and many less than a day. Binaries with periods of less than a few days are capable of merging

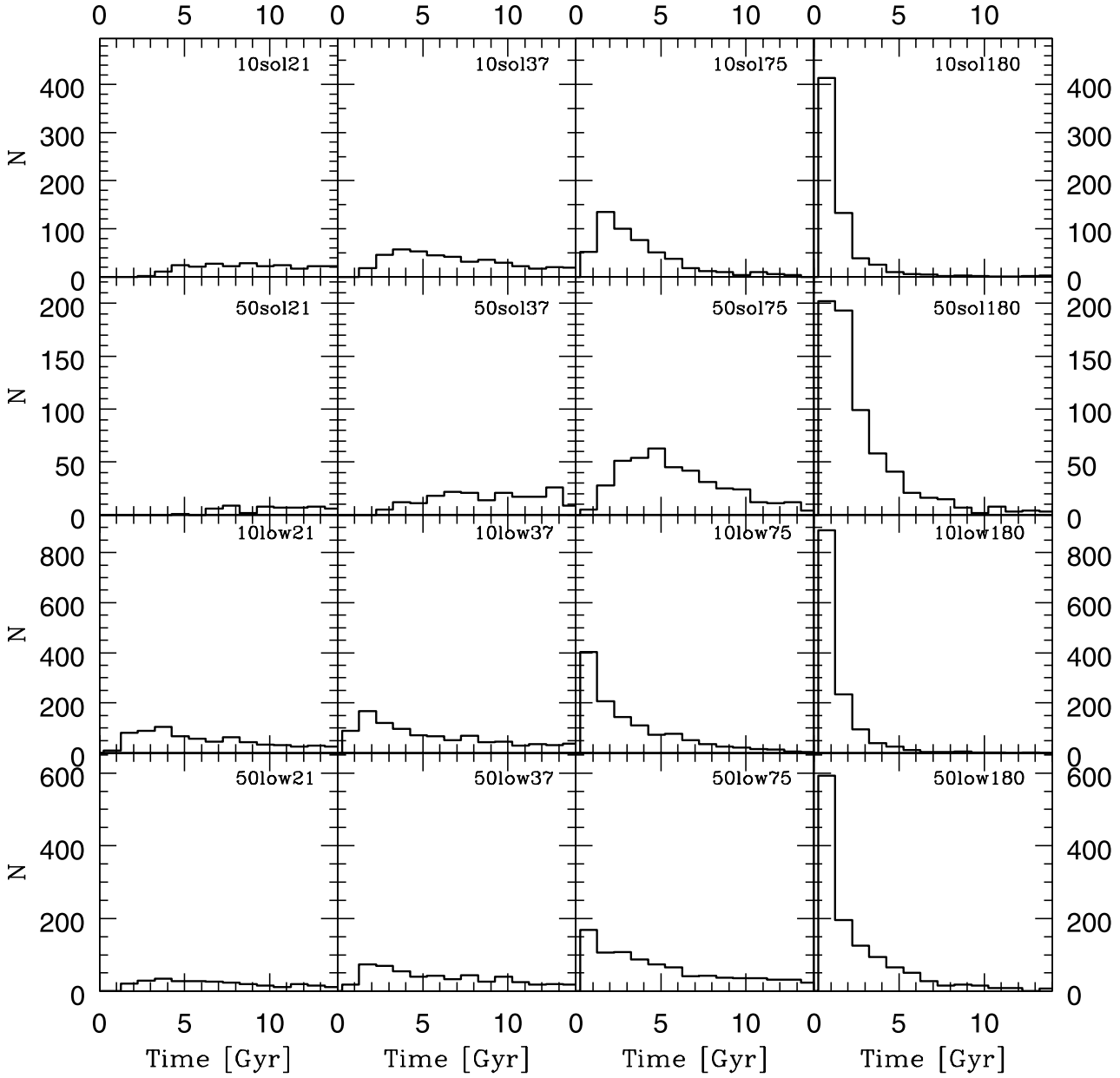

Figure 1. The number of BH–BH escapers per Gyr. Each panel gives the results for one set of initial conditions summed over all 10 independent realizations.

within a Hubble time due to gravitational radiation (Peters 1964) and are thus potential sources for ground-based detectors. Furthermore, unlike the binaries that remain within the cluster, these binaries will not be subject to disruption in further interactions, which prevented mergers within the cluster as described in Paper I. There is little variation in the period distribution with cluster parameters other than a tendency towards shorter periods in high-density clusters. This tendency is because the velocity dispersion, and thus the kinetic energy, is higher in these clusters. This means that a binary must be more energetic and thus shorter period in these clusters in order to survive.

In Fig. 4 we also present the period distribution on escape of BH–BH binaries that will merge within a Hubble time (see Section 4 for calculation of the merger time-scale). In general, the shorter period end of the escaper period distribution produces the mergers. This is not surprising since these binaries are closer and therefore more strongly affected by gravitational radiation. It is not, however, an absolute correlation since some longer period binaries merge and some short-period binaries do not. This is a result of both eccentricity and escape time. A long-period binary with a high eccentricity that escapes from a young cluster may merge in a Hubble time while a short-period, circular binary that escapes from an old cluster may not have time to merge. The trend towards short periods is weaker in the case of a thermal eccentricity distribution and the number of mergers is higher due to the preference for higher eccentricities and consequently shorter merger times. The difference in merger distribution with eccentricity distribution is not, however, very strong, especially in the high-concentration clusters.

Finally in Fig. 5, we show the chirp masses $M_{\rm chirp}$ of all BH–BH binaries at the time of escape as well as for all BH–BH mergers (see Section 4). The chirp mass,

$$M_{\rm chirp} = \frac{(m_1 m_2)^{3/5}}{(m_1 + m_2)^{1/5}}, \tag{3}$$

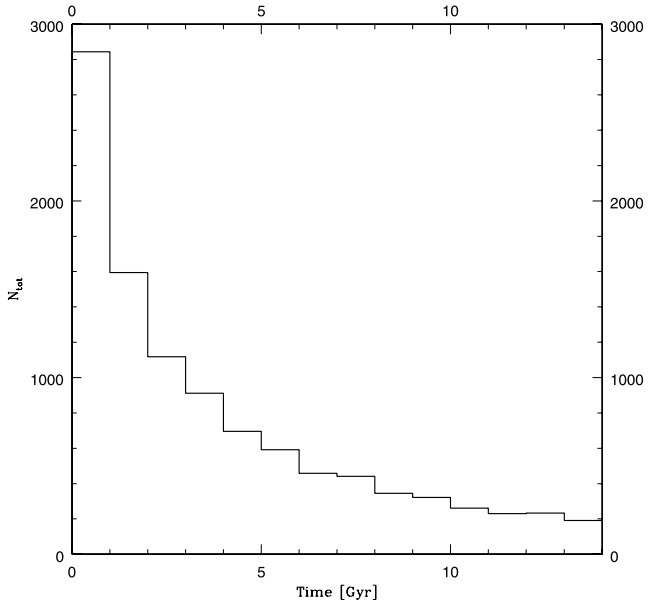

Figure 2. The total number of BH–BH escapers per Gyr summed over all 160 simulations.

where m_1 is the mass of the primary and m_2 is the mass of the secondary, is an important quantity in gravitational wave studies since the amplitude of a gravitational wave, h_0, is proportional to $M_{\rm chirp}$ (Pierro et al. 2001):

$$h_0 \propto \frac{G^{5/3}\omega^{2/3}M_{\rm chirp}^{5/3}}{rc^4}, \tag{4}$$

where ω is the angular frequency of the binary, r is the distance from the binary to the observer, and c is the speed of light. Thus, it is $M_{\rm chrip}$ rather than the total mass that is important for gravitational wave detection. $M_{\rm chirp}$ is larger for the low-metallicity systems due to the aforementioned higher mass of BHs produced by lower metallicity progenitors. It is also clear that in the low-metallicity cases the binaries with the highest chirp mass escape first. This is another consequence of mass segregation since the high-mass BH–BH binaries in the core will interact and be ejected more rapidly than their lower mass counterparts. This is not apparent in the high-metallicity cases, since there the spread in mass is not sufficient for this effect to be important (see Paper I). It is worth noting, however, that the time dependence of escaper chirp mass does not translate into a time-dependent merger chirp mass for any choice of initial conditions nor for either eccentricity distribution. This is due to the time lag between the escape of a BH–BH binary and its merger in the field. A short-period, low-mass binary may still merge before a long-period, high-mass binary. This will be explored in Section 4.

4 BH–BH MERGERS

Here we calculate the number of escaping BH–BH binaries that will merge within a Hubble time and when the merger will occur. We use the formalism presented in Peters & Mathews (1963) and Peters (1964) in order to calculate the gravitational wave inspiral time-scale for the BH–BH binaries. In this approximation, the field equations are linearized and the gravitational wave radiation is calculated in a multipole expansion. The first non-zero order in this expansion is the quadrupole term, which can be used to calculate the energy and angular momentum carried away from the binary by gravitational waves. This can then be used to calculate the effect of gravitational radiation on the orbital elements of the binary. The orbit-averaged changes in semimajor axis, a, and eccentricity, e, in the quadrupole approximation are

$$\langle \dot{a} \rangle = -\frac{64}{5}\frac{G^3}{c^5}\frac{m_1 m_2 (m_1+m_2)}{a^3(1-e^2)^{7/2}}\left(1+\frac{73}{24}e^2+\frac{37}{96}e^4\right) \tag{5}$$

and

$$\langle \dot{e} \rangle = -\frac{304}{15}e\frac{G^3}{c^5}\frac{m_1 m_2 (m_1+m_2)}{a^4(1-e^2)^{5/2}}\left(1+\frac{121}{304}e^2\right) \tag{6}$$

(Peters & Mathews 1963; Peters 1964). For each escaping binary, we solve equations (5) and (6) using a fourth-order Runge–Kutta integrator with time-steps chosen such that there is never more than a 1 per cent change in a. We integrate from the time of escape from the cluster until either the binaries merge or 1 $T_{\rm H}$ is reached. This gives us both an inspiral time-scale for the binary and, after each time-step, a self-consistently generated, quasi-static set of orbital parameters.

In Table 1 we show the number of escaping BH–BH binaries that merge within a Hubble time. The total number of BH–BH mergers tracks the total number of BH–BH escapers, however the proportion of escaping BH–BH binaries that merge within a Hubble time increases in clusters with low metallicity and high initial concentration. The correlation with metallicity is again due to the larger mass of BHs in the low-metallicity simulations and the correspondingly stronger gravitational wave radiation. The correlation with initial concentration is due to the fact that binaries tend to have shorter periods in clusters with a high concentration and thus have a shorter distance over which to inspiral and merge. As expected, the higher eccentricities in the thermal distribution lead to a larger number of mergers, a factor of $\sim$2 for individual clusters and $\sim$2–3 overall. Again there is relatively little simulation-to-simulation scatter in the number of mergers.

Fig. 6 shows the number of mergers for each set of initial conditions per Gyr where the time of merger of a BH–BH binary is given relative to the start of the simulation that produced it. The overall shapes broadly follow those found for the number of escapers per Gyr in Fig. 1 but with a time delay between when the peak number of escapers and the peak number of mergers is found. The mergers are delayed because inspiral in the galactic field is not an instantaneous process and it can take a binary several Gyr to merge. Again assuming that all star clusters form at the same time early in the life of the Universe, then the merger rate in the early Universe will be dominated by BH–BH binaries originating from dense, low-metallicity clusters, whereas at the current age of the Universe clusters of all types will be contributing mergers in similar numbers. The thermal eccentricity distribution does not appear to change this, and the time evolution of the merger rates in Fig. 6 is very similar for both distribution. In Fig. 7 we present the total number of mergers per Gyr summed over all realizations of all initial conditions. The profile is flatter than for the total number of escapers in Fig. 2, but still shows a peak in the merger rate while the cluster population is young. This implies that if we can detect BH–BH mergers at large redshift, then mergers from young clusters in the early Universe will dominate the detection rate. It also indicates that if dense, low-metallicity clusters form later in the universe they will be major contributors to the local BH–BH merger rate. The thermal eccentricity increases the total number of mergers but again the time evolution of the merger rate is largely unaffected.

Fig. 8 gives the inspiral time-scale for each BH–BH binary from the time of escape from the cluster until the merger as a function of

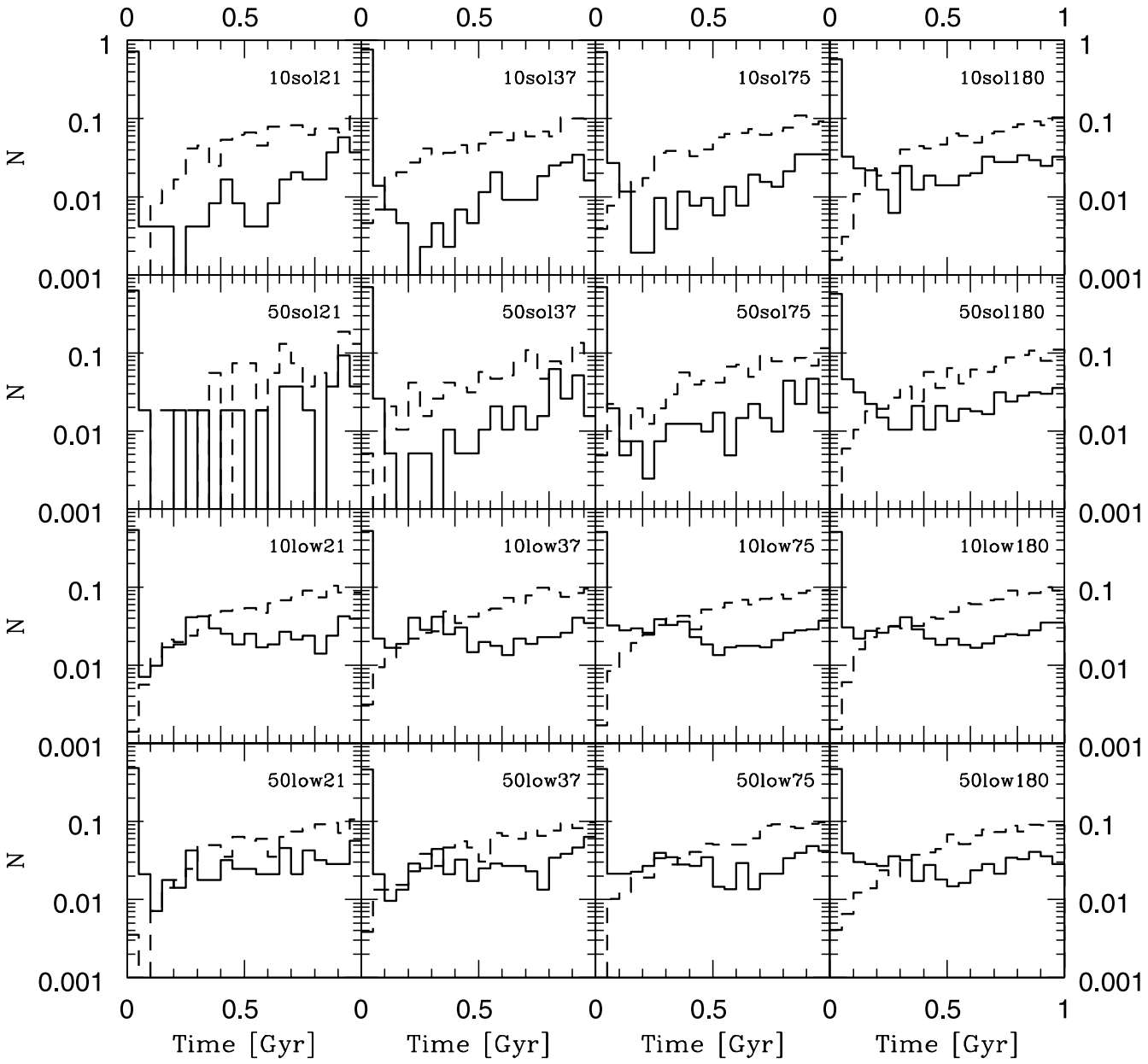

Figure 3. The eccentricity distribution of BH–BH escapers. Each panel gives the results of one set of initial conditions summed over all 10 independent realizations. The solid histogram is the distribution given by the Monte Carlo code, while the dashed histogram gives eccentricities drawn from a thermal distribution.

time of escape from the cluster. There are no clear trends in inspiral time as a function of escape time in any of the simulations for either eccentricity distribution. This implies that there is no clear link between merger time and escape time and that it is probably impossible to derive an escape rate from an observed merger rate. It also explains why there is no evolution in $M_{\rm chirp}$ of mergers as a function of time. High $M_{\rm chirp}$ binaries with a relatively long period that escape early are as likely as low $M_{\rm chirp}$ binaries with a short period that escape late. Thus the trend in the early escape of high $M_{\rm chirp}$ binaries does not translate into a similar trend in the merger rate.

5 DETECTION RATES

Now we must determine if the BH–BH mergers that are produced by our simulations can be detected by gravitational wave observatories. We follow the approach of O'Leary et al. (2006) who estimate the detectability of a BH–BH merger by comparing it to a template merger with a known signal-to-noise ratio at a given distance. A merger with a redshifted chirp mass of $\mathcal{M}_{\rm chirp} = (1 + z_{\rm m})M_{\rm chirp}$, where $z_{\rm m}$ is the redshift of the merger, is considered detectable at a luminosity distance $D_{\rm L} = (1 + z_{\rm m})D_{\rm prop}$, where $D_{\rm prop}$ is the proper distance to the merger, if (O'Leary et al. 2006)

$$\frac{D_{\rm L,0}}{D_{\rm L}}\left(\frac{\mathcal{M}_{\rm chirp}}{\mathcal{M}_{\rm chirp,0}}\right)^{5/6}\sqrt{\frac{s(f_{\rm off})}{s(f_{\rm off,0})}} > 1, \quad (7)$$

where $D_{\rm L,0}$ is the luminosity distance at which a merger of redshifted chirp mass $\mathcal{M}_{\rm chirp,0}$ is known to be detectable at a given signal-to-noise ratio. For the planned advanced detectors, it is estimated that a equal mass NS–NS binary with $M_{\rm chirp} = 1.2\,{\rm M}_{\odot}$ can be detected with a signal-to-noise ratio of 8 at a distance of $\sim$190 Mpc

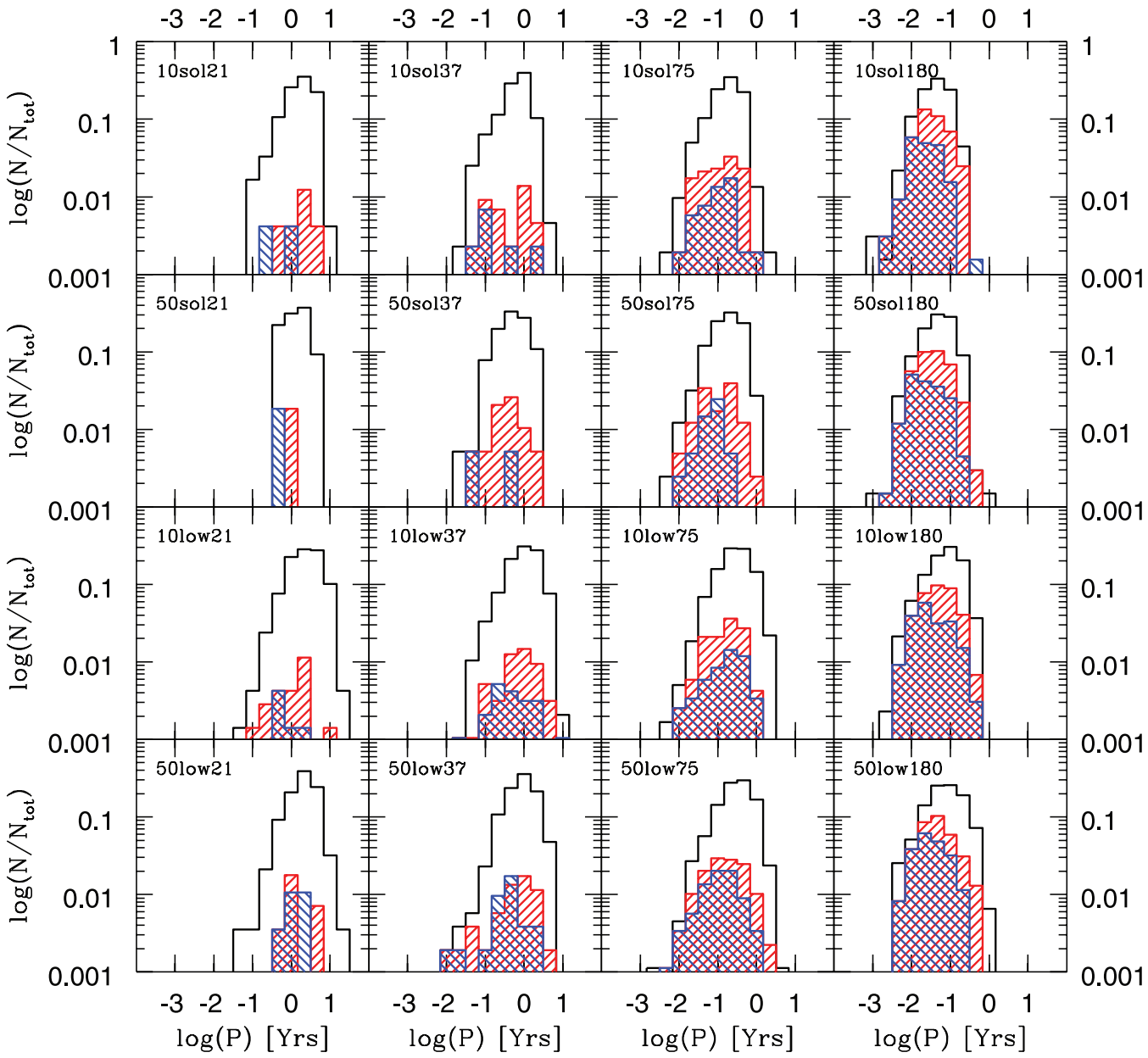

Figure 4. The period distribution of BH–BH escapers binned uniformly in log space. Each panel gives the results of one set of initial conditions summed over all 10 independent realizations. The black histogram gives the period distribution of all BH–BH escapers. The blue filled histogram gives the period distribution at escape of all BH–BH escapers that merge within a Hubble time. The red filled histogram also gives the period distribution at escape of all BH–BH escapers that merge within a Hubble time but using eccentricities at escape drawn from a thermal distribution rather than those produced by the Monte Carlo code.

(Harry 2005; O'Shaughnessy et al. 2005). The distance for the current generation of detectors is some 10 times lower. The detector response function, $s(f_{\rm off})$, is given by (O'Leary et al. 2006)

$$s(f_{\rm off}) = \int_0^{f_{\rm off}} \frac{(f')^{-7/3}}{S_{\rm N}(f')}\,{\rm d}f', \tag{8}$$

where $S_{\rm N}(f')$ is the noise spectrum of the detector. For ease of comparison, we use the same approximation as used by Cutler & Flanagan (1994) and O'Leary et al. (2006):

$$S_{\rm N}(f') \propto \begin{cases} \infty, & f' < 10{\rm Hz} \\ \left(\dfrac{f_0}{f'}\right)^4 + 2\left[1 + \left(\dfrac{f'}{f_0}\right)^2\right], & f' \geq 10{\rm Hz}, \end{cases} \tag{9}$$

with $f_0 = 70\,{\rm Hz}$. A constant of proportionality is not required in equation (9) because it will cancel out in equation (7). The cut-off frequency, $f_{\rm off}$, is the frequency at which the merger occurs and detailed relativistic modelling becomes necessary. For the reference inspiral we use the estimate of Cutler & Flanagan (1994) which yields $f_{\rm off,0} \sim 720\,{\rm Hz}$ for the NS–NS reference binary we have chosen. For the BH–BH inspiral the frequency is generally taken to be that of the last circular orbit before the final plunge. We use the same circular estimate as O'Leary et al. (2006):

$$f_{\rm off} \approx 200 \left(\frac{20\,{\rm M}_\odot}{M}\right)\left(\frac{1}{1+z_{\rm m}}\right){\rm Hz}, \tag{10}$$

where M is the total mass of the inspiralling binary.

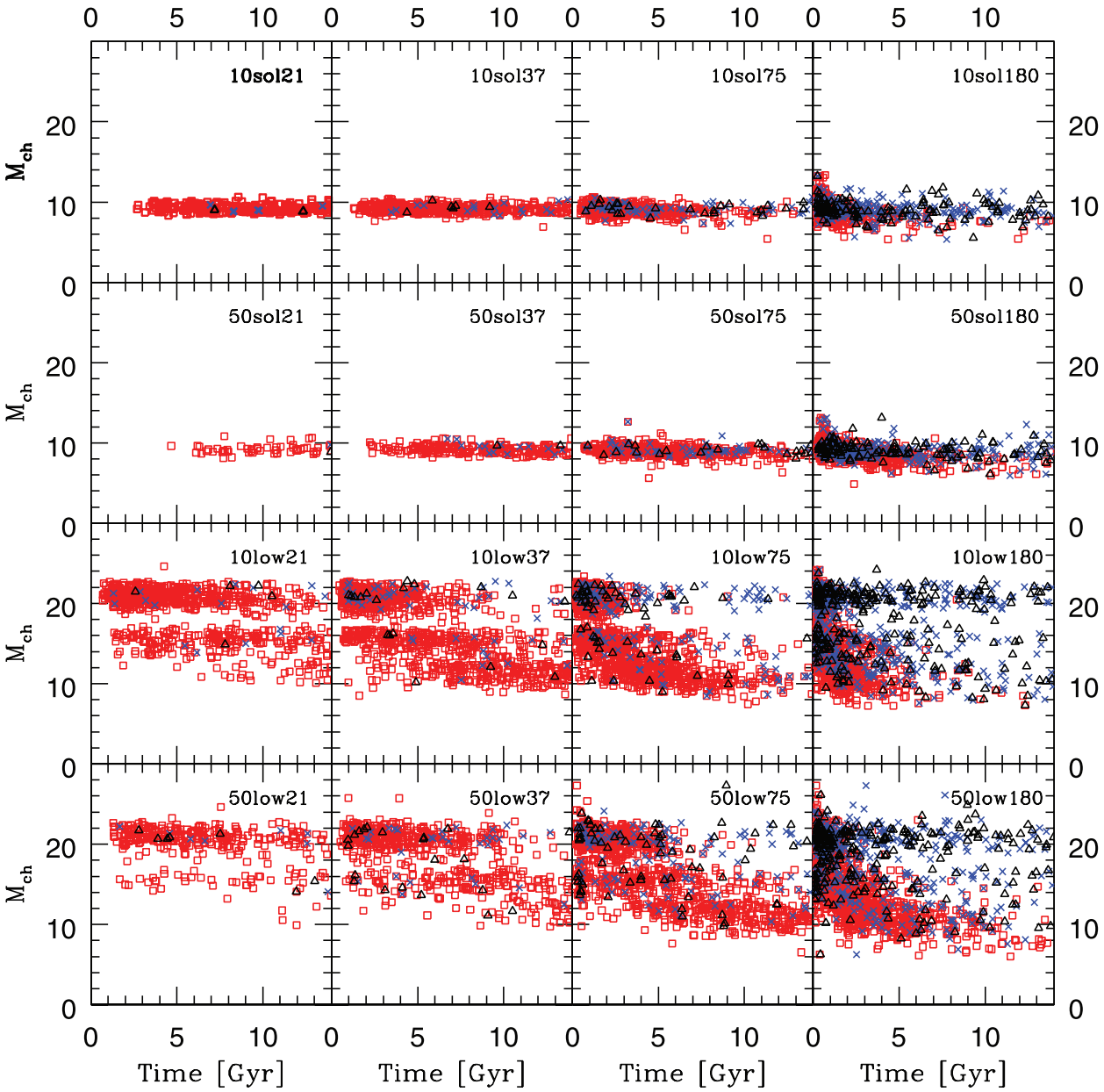

Figure 5. $M_{\rm chirp}$ for BH–BH binaries at the time of escape from the cluster (red open squares), BH–BH mergers (black open triangles) and BH–BH mergers with initial eccentricities drawn from a thermal distribution (blue crosses). Each panel shows all binaries from all 10 independent realizations of one set of initial conditions.

From our simulations, we have $M_{\rm chirp}$ for each of our mergers and the time of the merger relative to the start of the simulation. By assuming a formation time, $T_{\rm form}$, for each simulation relative to the age of the Universe, we can calculate a look-back time, redshift and proper distance to the merger and use equation (7) to determine if the merger can be detected. To convert this to a merger rate per year for ground-based detectors, we must make assumptions about the formation history and density of globular clusters in the Universe. For simplicity, we assume that all globular clusters form in a single burst at some time $T_{\rm form}$ in the past. Again for simplicity we assume a constant number density of $n_0 \approx 8.4h^3$ clusters Mpc^{-3}. This estimate comes from Portegies Zwart & McMillan (2000) and is based on observations of the local Universe taking into account the different specific frequencies of clusters in galaxies of different Hubble types. We then bin the detections in uniform bins in look-back time, calculate the proper distance, $D_{{\rm prop},i}$, to the edge of each bin, and use the equation (O'Leary et al. 2006)

$$R_{\rm det} = \sum_{i=1}^{100} \frac{N_i}{\Delta t} \frac{4\pi}{3} n_0 \left(D^3_{{\rm prop},i} - D^3_{{\rm prop},i-1}\right) (1+z_i)^{-1} \qquad (11)$$

to calculate the detection rate. N_i is the number of detections calculated from our simulation in bin i, Δt is the bin width and the factor $(1+z_i)^{-1}$ comes from the cosmological time dilation of the detection rate. We use the cosmological parameters $h = 0.72$, $\Omega_{\rm m} = 0.27$ and $\Omega_{\rm Lambda} = 0.73$. We note that it would be possible in principle to perform a more careful estimate of the density of globular clusters in the Universe by using Press–Schechter formalism and making assumptions about the baryon fraction per halo, the fraction of baryons that become globular clusters, the evolution of the globular cluster mass function and globular cluster formation rate.

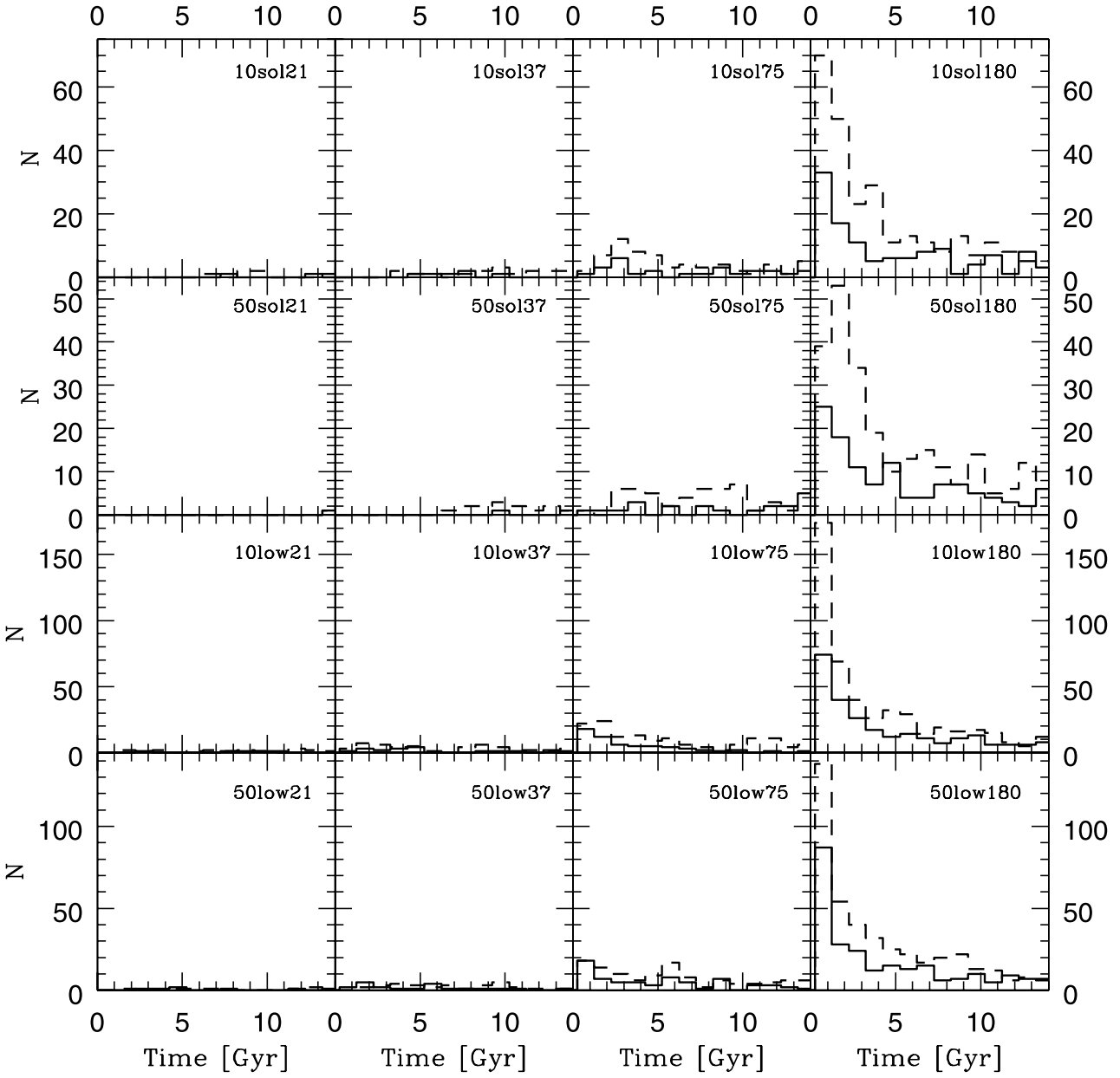

Figure 6. Merger rates for BH–BH escapers binned per Gyr. Each panel gives the merger rate for one choice of initial conditions summed over all 10 independent realizations. The solid histograms give the merger rate using the eccentricity distribution produced by the Monte Carlo code, while the dashed histograms give the rate using eccentricities drawn from a thermal distribution.

This would, however, introduce a large number of uncontrolled parameters into our modelling and since our simulations do not cover the whole range of globular cluster masses convolving them with the evolution of the globular cluster mass function seems unjustified. For these reasons, we will limit ourselves to simple assumptions about the globular cluster population in the Universe and save more detailed modelling of the cluster population for when we have a larger set of simulations.

In Fig. 9 we present the detection rate per year as a function of look-back time to the assumed formation event. We have chosen a look-back time to $T_{\rm form}$ to be between 1 and 13 Gyr. We have also calculated rates for three different detector sensitivities (parametrized by $D_{\rm L,0}$). The dotted line represents the advanced generation of detectors [parameters chosen to roughly correspond with LIGO for comparison with O'Leary et al. (2006) and Sadowski et al. (2008)] with the solid line representing a detector 10 times less sensitive (corresponding roughly to the detectors currently in operation) and the dashed line corresponding to a detector 10 times more sensitive. For the current generation of detectors, there is a very low probability of detection, normally a rate of less than 0.1 events $\rm yr^{-1}$. The current detectors are not sensitive enough to detect mergers out to cosmological distances and thus probe a volume that is too small to contain many mergers. By contrast, the prospects for the advanced detectors are much better with most clusters promising detection rates of more than 1 $\rm yr^{-1}$ and some of the most optimistic providing $\sim$100 detections $\rm yr^{-1}$. The advanced detection rate demonstrates some interesting trends with formation time. The low-density, high-metallicity simulations only produce detections if the clusters are assumed to form very early in the Universe. This is because these clusters evolve slowly and do not produce BH–BH mergers until

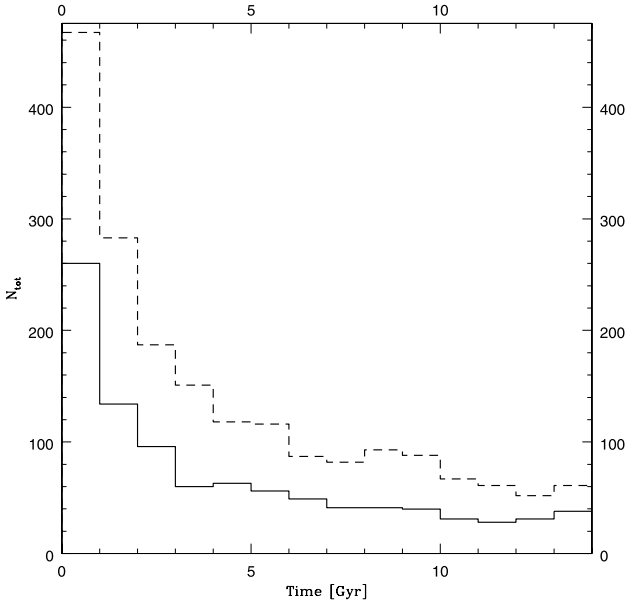

Figure 7. The number of BH–BH merger binned per Gyr and summed over 160 all realizations of all initial conditions. The solid black line gives the results if the binaries have the eccentricities from the Monte Carlo code, while the dashed line gives the result if the binaries have eccentricities drawn from a thermal distribution.

late in their lives (see Fig. 6). By contrast, according to Fig. 6, the higher density, lower metallicity clusters evolve much more rapidly and can provide a significant detection rate even if they formed quite recently. Indeed, these clusters produce a peak detection rate for $T_{\rm form} \sim 5$–6 Gyr. The peak at 5–6 Gyr comes form the balance between detection volume and detectability. For formation times less than 5–6 Gyr ago, the advanced detectors will be able to detect all mergers, and by choosing an earlier formation time the volume of space in which globular clusters exist, and thus the number of globular clusters, increases and the detection rate goes up. Clusters that form more than ∼6 Gyr ago are sufficiently distant that even the next generation of detectors cannot detect all of the events and in particular the early burst of mergers moves out of the detection range. Thus the detection rate starts to fall again. For a sensitivity 10 times greater (currently well beyond our technical capabilities) we would be able to detect all mergers at very large distances, and thus the detection rate continues to increase with detection volume up to a $T_{\rm form}$ of ∼10 Gyr. The choice of eccentricity distribution does not affect the shape of the curves in Fig. 9, only the expected detection rate at a given time. Furthermore, the detection rate is increased by a factor of only ∼2–3. This is fully consistent with the previous plots that show the thermal eccentricity distribution changes the total number of mergers by a factor of ∼2–3, but does not change the time at which the mergers occur or any of their other properties.

Fig. 10 gives the detection rate assuming that all of our simulated clusters are present in the Universe in equal numbers. The shape is very similar to that of the low-metallicity, high-density clusters, indicating that it is these clusters that will dominate the detection rate. The overall detection rate is, however, somewhat lower than for these clusters. The most optimistic detection rates for the current generation of detectors are $\sim 0.08\,{\rm yr}^{-1}$ for the Monte Carlo eccentricity distribution and $\sim 0.15\,{\rm yr}^{-1}$ for the thermal distribution. For the advanced detectors, the rate drops to a peak of $\sim 15\,{\rm yr}^{-1}$ for the Monte Carlo distribution and ∼29 for the thermal distribution. This is because the clusters that produce few mergers serve only to dilute the detection rate. 15 BH–BH detections per year is, however, still several times that predicted by Belczynski et al. (2007) for galactic field populations, and thus star clusters provide a significant enhancement to the BH–BH detection rate.

6 DISCUSSION

As previously mentioned, the investigations of O'Leary et al. (2006) and Sadowski et al. (2008) are some of the most complete available and make opposing dynamical assumptions regarding mass segregation of BHs. In the work of O'Leary et al. (2006), BHs are assumed to mass segregate completely and form a strongly interacting subsystem in the core of the cluster. This leads to a large number of interactions that can both create and destroy BH–BH binaries. By contrast, Sadowski et al. (2008) assume that the BHs remain in thermal equilibrium with the rest of the stars in the cluster. This leads to a much lower interaction rate between the BHs and, consequently, a lower rate of both BH–BH formation and destruction. In practice, the lower destruction rate wins and the simulations of Sadowski et al. (2008) predict a yearly detection rate of the orders of magnitude higher than that of O'Leary et al. (2006). This implies that the predictions of O'Leary et al. (2006) represent a lower limit on the BH–BH merger detection rate, while those of Sadowski et al. (2008) represent an upper limit. O'Leary et al. (2006) also predict that up to 70 per cent of BH–BH mergers will occur in binaries that have been ejected from the cluster, whereas Sadowski et al. (2008) predict that ∼90 per cent of mergers occur in binaries remaining within the clusters.

The predictions of our simulations, using a fully self-consistent treatment of stellar dynamics, agree with those of O'Leary et al. (2006) better than those of Sadowski et al. (2008) for both eccentricity distributions. In Paper I we showed that the BHs are strongly mass segregated with the half-mass radius of the BH system more than 10 times smaller than the half-mass radius of the entire system in all simulations (see fig. 3 of Paper I). The very high interaction and disruption rate for BH–BH binaries (much higher than for other objects in the simulations) indicates that this subpopulation is strongly interacting. This is in qualitative agreement with the assumption of complete mass segregation in O'Leary et al. (2006). We confirm that few, if any, mergers should take place within the clusters and the peak detection rates predicted for our clusters in Fig. 9 fall in the same range as or are only slightly higher (a factor of 2–4) than those given in table 2 of O'Leary et al. (2006). This agreement is in spite of the fact that both O'Leary et al. (2006) and Sadowski et al. (2008) use a similar and much more detailed treatment of few-body interactions than is present in our Monte Carlo code. For these reasons, we favour the approximations made by O'Leary et al. (2006) rather than those made by Sadowski et al. (2008) and postulate that a proper treatment of global globular cluster dynamics is at least as important in predicting event *rates* for ground-based detectors as is the detailed microphysics of the interactions.

The most significant difference between our predictions and those of O'Leary et al. (2006) is that we do not find any mergers between BH–BH binaries that remain in our clusters, only in the escapers. As we demonstrated in Paper I, this is because in our clusters BH–BH binaries tend to either be disrupted or ejected by dynamical interactions before they have a chance to merge due to gravitation wave radiation. It is possible that this effect is real, as suggested by the results of both Portegies Zwart & McMillan (2000) and Banerjee et al. (2010), however it may also be due to our more approximate treatment of few-body interactions. As discussed in Paper I, we

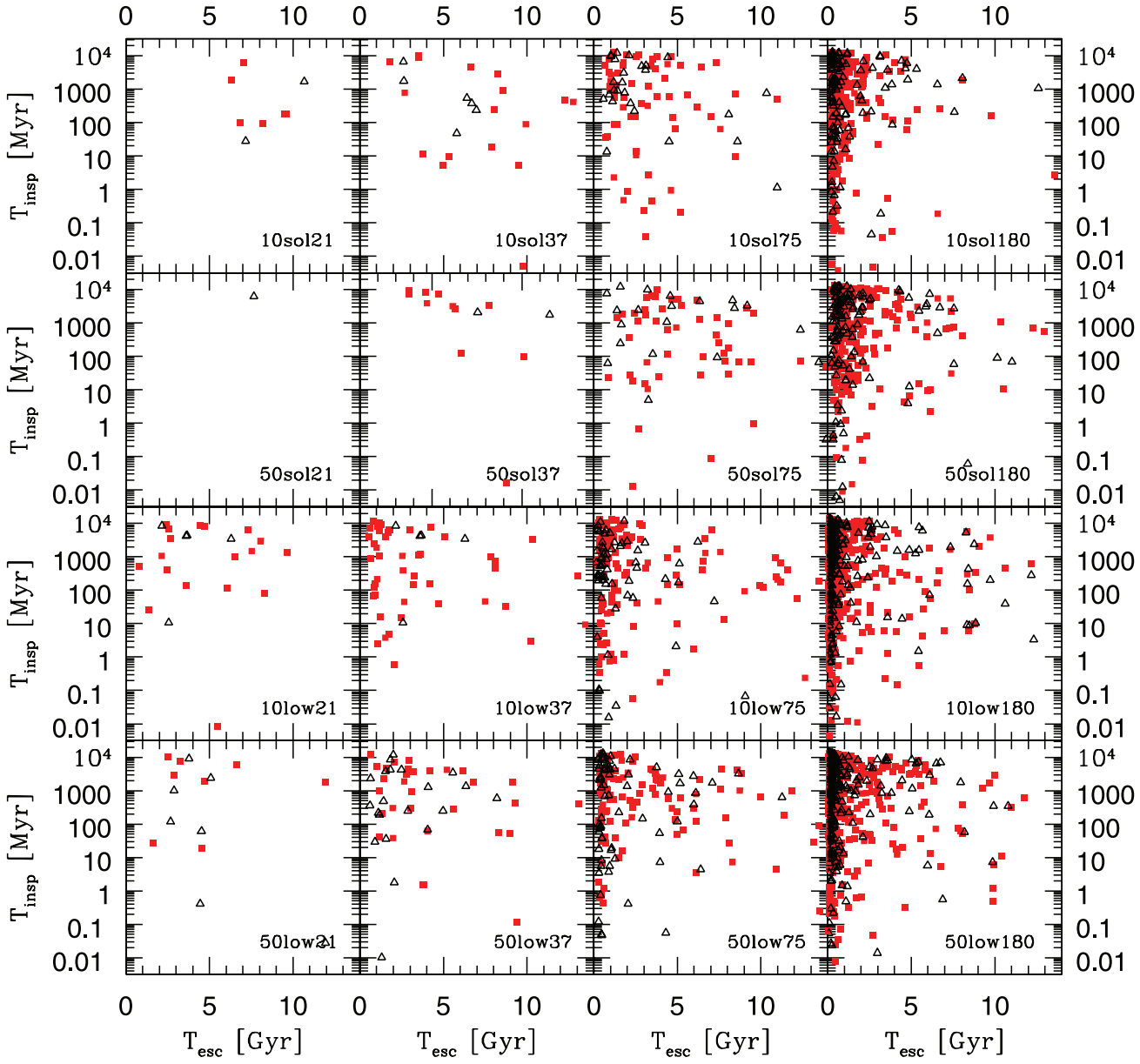

Figure 8. The merger time-scale as a function of escape time for all escaping BH–BH binaries that merge. Black triangles give the times for binaries with eccentricities taken from the Monte Carlo simulation, while red squares give the times for binaries with eccentricities drawn from a thermal distribution. Each panel shows the binaries from all realizations of one set of initial conditions.

may be overestimating both the disruption rate in binary–binary interactions and the velocity kick applied to the centre of mass of each member of an interaction while at the same time underestimating the eccentricities of binaries formed through these interactions. This combination of effects would lead to shorter disruption time-scales, larger escape probabilities and longer gravitational wave inspiral time-scales than would be expected in a real cluster. Thus it is almost certain that our merger rates, particularly those within the cluster, are lower limits. A version of our Monte Carlo code with a more detailed treatment of few-body interactions is currently in development and will allow us to investigate our BH–BH escape rates in more detail.

We note in passing that during their inspirals, many of our BH–BH binaries pass through the LISA frequency band. Although normally only considered a source of confusion-limited noise, several authors (Hils, Bender & Webbink 1990; Benacquista 2001; Nelemans et al. 2001; Kocsis et al. 2006; Belczynski et al. 2010; Downing et al. 2010) have considered the possibility that strong stellar mass sources may be individually resolved by LISA. Unlike supermassive BH binaries, stellar mass binaries would not be visible to cosmological distances due to their lower masses. In Fig. 11 we show the expected signal strength for a binary consisting of two 20 $M_{\odot}$ BHs at various distances. The amplitude of the gravitational wave signal of the binary is calculated according to equation (3) of Belczynski et al. (2010), and the sensitivity curve is computed using the Larson, Hellings & Hiscock (2002) LISA sensitivity curve generator for a one-year observation at a signal-to-noise ratio of 1. Fig. 11 implies that stellar mass BH–BH binaries may be individually resolvable both within our own Galaxy and throughout the Local Group. The possibility of detecting a stellar mass source with LISA at such

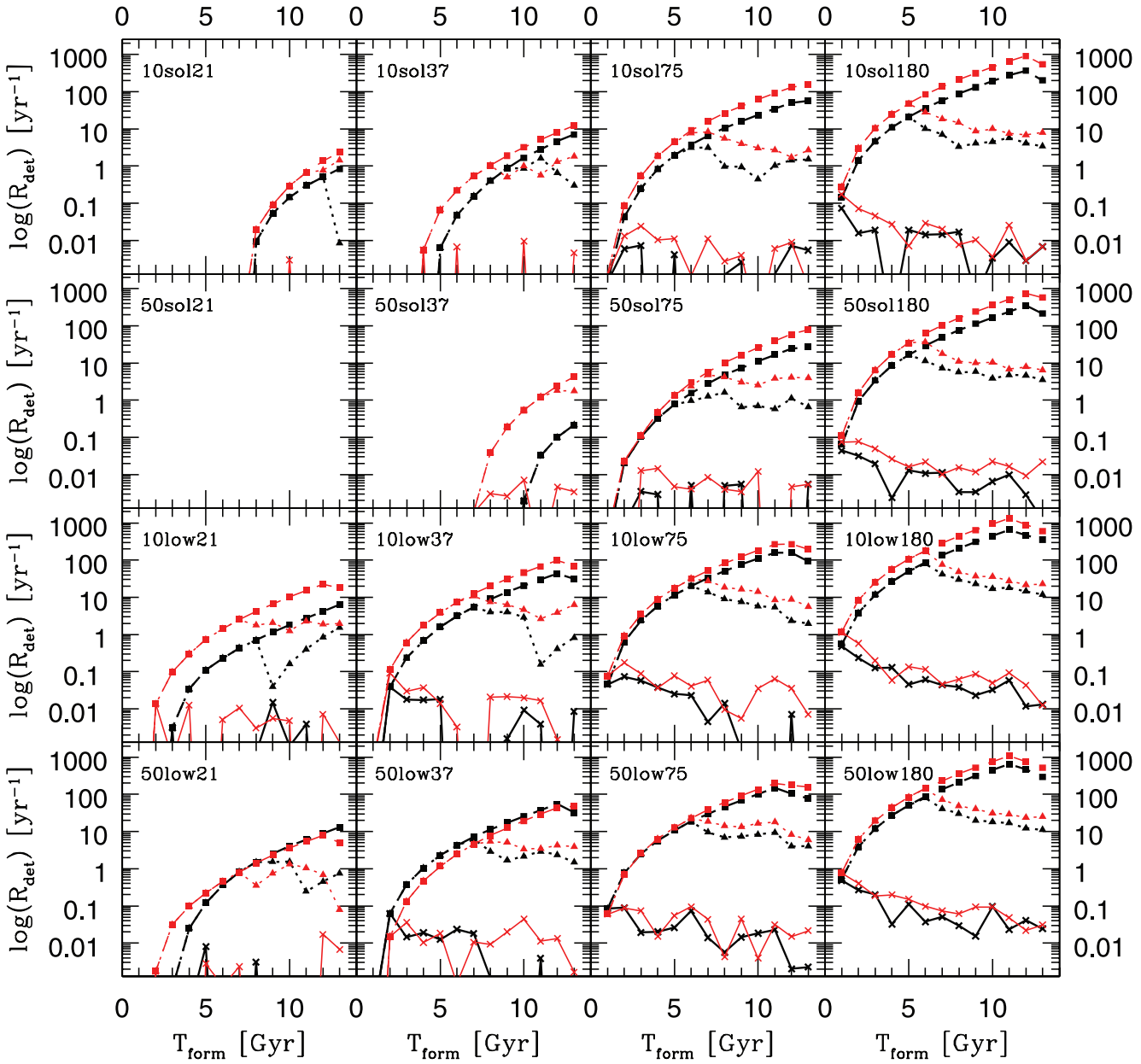

Figure 9. Detection rates by cluster type. Each panel gives the expected detection rate if the entire cluster population in the Universe was composed of identical clusters, each with the corresponding initial conditions. The x-axis gives the look-back time to $T_{\rm form}$ in Gyr. The solid line with crosses is for $D_{\rm L,0} = 19.1$ Mpc, the dotted line with triangles is for $D_{\rm L,0} = 191.0$ Mpc and the dashed line with squares is for $D_{\rm L,0} = 1910.0$ Mpc. Black lines give the detection rates if the binaries have the eccentricities produced by the Monte Carlo code, while the red lines give the rate if the binaries have eccentricities drawn from a thermal distribution.

distances is interesting, but estimating the expected event rate will require more detailed modelling of the globular cluster population in the local Universe. We defer a detailed study of this possibility to a future publication.

7 CONCLUSIONS

We have studied the behaviour of the BH population in globular clusters, focusing on BH–BH binaries formed by dynamical interactions but then inspiralling and merging in a galactic field. We find that globular clusters produce such binaries quite efficiently and should significantly enhance the BH–BH binary detection rate for the next generation of ground-based detectors. This enhancement is in line with the predictions of O'Leary et al. (2006) rather than the more extreme factors predicted by Sadowski et al. (2008). In future, we plan to include few-body integration in our code and see if we get better agreement with O'Leary et al. (2006) on the number of mergers within clusters. Given the possibility of a stellar mass LISA detection at extragalactic distances, we are also interested in extending our study to other Local Group galaxies with simulations chosen to more closely match the real globular cluster population. We conclude that star clusters can efficiently enrich galactic fields with BH–BH binaries and must be taken into account when estimating detection rates and population characteristics for gravitational wave detectors.

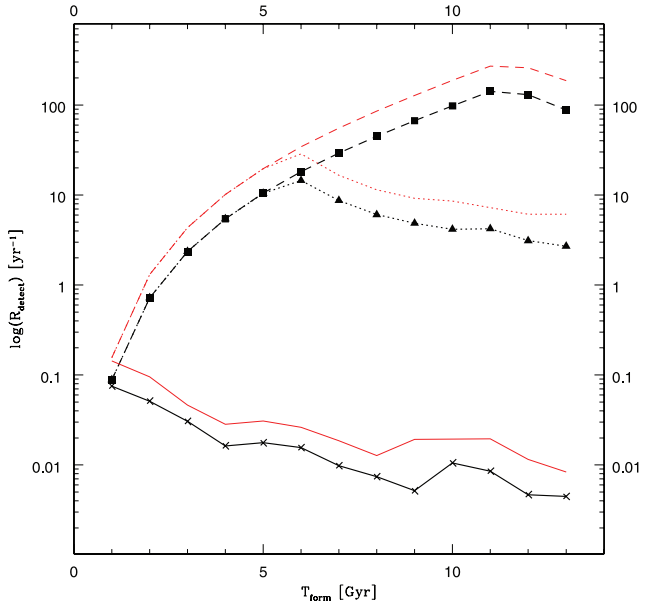

Figure 10. The detection rate assuming all types of clusters are present equally in the Universe with an overall number density of $n_0 = 8.4h^3\,\mathrm{Mpc}^{-3}$. The solid lines with crosses are for $D_{\mathrm{L},0} = 19.1$ Mpc, the dotted lines with triangles for $D_{\mathrm{L},0} = 191.0$ Mpc and the dashed lines with squares for $D_{\mathrm{L},0} = 1910.0$ Mpc. Black lines give the detection rate if the binaries have the eccentricities produced by the Monte Carlo code, while the red lines give the rate if the binaries have eccentricities drawn from a thermal distribution.

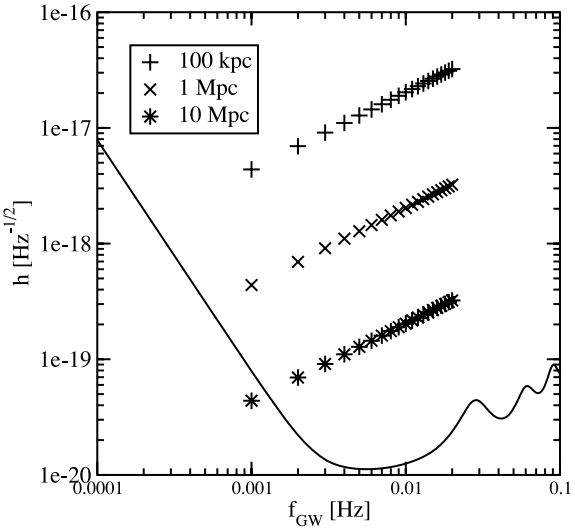

Figure 11. Signal strengths of a BH–BH system containing two $20\,\mathrm{M}_\odot$ BHs at 100 kpc, 1 and 10 Mpc, and frequencies between 1 and 10 mHz. The LISA sensitivity curve is computed for a one-year observation with a signal-to-noise ratio of 1.

ACKNOWLEDGMENTS

JMBD would like to thank the International Max-Planck Research School for Astronomy and Cosmic Physics at the University of Heidelberg (IMPRS-HD) for providing funding for his PhD, during which the main part of this work was carried out. JMBD also acknowledges continuing support from VESF grant EGO-DIR-50-2010. The simulations have been carried out at the High Performance Computing Centre Stuttgart (HLRS) using the resources of Baden-Württemberg grid (bwgrid) through the German Astrogrid-D and D-Grid projects. MJB acknowledges the support of NASA grant NNX08AB74G and the Center for Gravitational Wave Astronomy, supported by NSF award #0734800 and NASA award NNX09AV06A. MG was supported by Polish Ministry of Science and Higher Education through the grant 92/N.ASTROSIM/2008/0 and N N203 380036. RS thanks the Deutsches Zentrum für Luft- und Raumfahrt (DLR) for support within the LISA Germany project.

REFERENCES

Abbott B. (LIGO Scientific Collaboration) et al., 2005, Phys. Rev. D, 72, 082001
Abbott B. (LIGO Scientific Collaboration) et al., 2006, Phys. Rev. D, 73, 062001
Abbott B. (LIGO Scientific Collaboration) et al., 2010, Class. Quantum Grav., 27, 173001
Banerjee S., Baumgardt H., Kroupa P., 2010, MNRAS, 402, 371
Baumgardt H., 2001, MNRAS, 325, 1323
Belczynski K., Kalogera V., Bulik T., 2002, ApJ, 572, 407
Belczynski K., Sadowski S., Rasio F. A., Bulik T., 2006, ApJ, 650, 303
Belczynski K., Taam R. E., Kalogera V., Rasio F. A., Bulik T., 2007, ApJ, 662, 504
Belczynski K., Benacquista M., Bulik T., 2010, ApJ, 725, 816
Benacquista M., 2001, Class. Quantum Grav., 19, 1297
Benacquista M. J., DeGoes J., Lunder D., 2004, Class. Quantum Grav., 21, 509
Cutler C., Flanagan É. E., 1994, Phys. Rev. D, 49, 2658
Downing J. M. B., Benacquista M. J., Giersz M., Spurzem R., 2010, MNRAS, 407, 1946 (Paper I)
Evans C. R., Iben I., Smarr L., 1987, ApJ, 323, 129
Fryer C. L., Woosley S. E., Hartmann D. H., 1999, ApJ, 526, 152
Giersz M., 1998, MNRAS, 298, 1239
Giersz M., 2001, MNRAS, 324, 218
Giersz M., 2006, MNRAS, 371, 484
Giersz M., Heggie D. C., 2008, MNRAS, 389, 1858
Giersz M., Heggie D. C., 2009, MNRAS, 395, 1173
Giersz M., Spurzem R., 2003, MNRAS, 343, 781
Giersz M., Heggie D. C., Hurley J. R., 2008, MNRAS, 388, 429
Gültekin K., Miller M. C., Hamilton D. P., 2005, ApJ, 616, 221
Hansen B. M. S., Phinney E. S., 1997, MNRAS, 291, 569
Harry G., 2005, Material Downselect: Rational and Directions. Caltech, Pasadena (http://dcc.ligo.org/cgi-bin/DocDB/ShowDocument?docid=35642)
Heggie D. C., 1975, MNRAS, 173, 729
Heggie D. C., Giersz M., 2009, MNRAS, 397, 46
Heggie D. C., Hut P., McMillan S. L. W., 1996, ApJ, 467, 359
Hénon M., 1971, Ap&SS, 13, 284
Hills J. G., Fullerton L. W., 1980, AJ, 85, 1281
Hils D., Bender P. L., Webbink R. F., 1990, ApJ, 360, 75
Hobbs G., Lorimer D. R., Lyne A. G., Kramer M., 2005, MNRAS, 360, 974
Hurley J. R., Pols O. R., Tout C. A., 2000, MNRAS, 315, 543
Hurley J. R., Tout C. A., Pols O. R., 2002, MNRAS, 329, 897
Kalogera V. et al., 2004, ApJ, 601, L179
Khalisi E., Amaro-Seoane P., Spurzem R., 2007, MNRAS, 374, 703
Kocsis B., Gáspár M. E., Márka S., 2006, ApJ, 648, 411
Kroupa P., 1995, MNRAS, 277, 1507
Kroupa P., Tout C. A., Gilmore G., 1993, MNRAS, 251, 293
Larson S. L., Hellings R. W., Hiscock W. A., 2002, Phys. Rev. D, 66, 062001
Lorimer D., 2008, Living Rev. Relativ., 11, 8
Lyne A. G., Lorimer D. R., 1994, Nat, 369, 127
Mikkola S., 1983a, MNRAS, 203, 1107
Mikkola S., 1983b, MNRAS, 205, 733
Mikkola S., 1984a, MNRAS, 207, 115
Mikkola S., 1984b, MNRAS, 208, 75
Nelemans G., Yungelson L., Portegies Zwart S. F., 2001, A&A, 375, 890

O'Leary R. M., Rasio F. A., Fregeau J. M., Ivanova N., O'Shaughnessy R., 2006, ApJ, 637, 937
O'Shaughnessy R., Kim C., Fragos T., Kalogera V., Belczynski K., 2005, ApJ, 633, 1076
Peters P. C., 1964, Phys. Rev., 136, 1224
Peters P. C., Mathews J., 1963, Phys. Rev., 131, 435
Pierro V., Pinto I., Spallicci A., Laserra E., Recano F., 2001, MNRAS, 325, 358
Portegies Zwart S. F., McMillan S. L. W., 2000, ApJ, 528, 17
Portegies Zwart S. F., Yungelson L. R., 1998, A&A, 332, 173
Ruiter A., Belczynski K., Benacquista M., Larson S., Williams G., 2010, ApJ, 717, 1006
Sadowski A., Belczynski K., Bulik T., Ivanova I., Rasio F. A., O'Shaughenessy R., 2008, ApJ, 676, 1162
Sigurdsson S., Phinney E. S., 1993, ApJ, 415, 631
Spitzer L., 1987, Dynamical Evolution of Globular Clusters. Princeton Univ. Press, Princeton, NJ
Stodółkiewicz J. S., 1982, Acta Astron., 32 63
Stodółkiewicz J. S., 1986, Acta Astron., 36, 19
Timpano S. E., Rubbo L. J., Cornish N. J., 2006, Phys. Rev. D, 73, 122001
Watters W. A., Joshi K. J., Rasio F. A., 2000, ApJ, 539, 331

This paper has been typeset from a TEX/LATEX file prepared by the author.